

方知库
Eco-Environmental
Knowledge Web

环境科学

ENVIRONMENTAL SCIENCE

ISSN 0250-3301 CODEN HCKHDV

HUANJING KEXUE

基于高分影像的城市水体遥感综合分级方法

杨子谦, 刘怀庆, 吕恒, 李云梅, 朱利, 周亚明, 李玲玲, 毕顺



■ 主办 中国科学院生态环境研究中心

■ 出版 科学出版社



2021年5月

第42卷 第5期

Vol.42 No.5

目次

北京冬季 PM_{2.5} 中有机气溶胶的化学特征和来源解析 徐楠, 王甜甜, 李晓, 唐荣志, 郭松, 胡敏 (2101)

北京地区 2019 年 2~3 月供暖结束后两次污染过程特征分析 尹晓梅, 蒲维维, 王继康, 刘湘雪, 乔林 (2110)

北京 2019 年冬季一次典型霾污染特征与成因分析 廉涵阳, 杨欣, 张普, 陈义珍, 杨小阳, 赵好希, 何友江, 赵丹婷 (2121)

青岛沿海地区夏季和冬季新粒子生成特征对比 孙悦, 朱玉姣, 孟赫, 刘兵, 刘玉虹, 董灿, 姚小红, 王文兴, 薛丽坤 (2133)

太原市城乡居民采暖季室内灰尘中重金属的污染特征及其生态风险评价 黄浩, 徐子琪, 严俊霞, 赵秀阁, 王丹璐 (2143)

西安市新装修公共场所空气污染物浓度分析及健康风险评价 范洁, 樊灏, 沈振兴, 党文鹏, 郑伟, 王志华, 付毅 (2153)

超低排放典型燃烧源颗粒物及水溶性离子排放水平与特征 胡月琪, 王铮, 郭建辉, 冯亚君, 丁萌萌, 颜旭 (2159)

合肥市夏季大气颗粒物中微生物群落的高通量测序分析 姜少毅, 孙博文, 代海涛, 王润芳, 马大卫, 朱仁斌 (2169)

郑州市细颗粒物时空差异及管控措施影响 董喆, 袁明浩, 苏方成, 张剑飞, 孙佳侯, 张瑞芹 (2179)

2016~2019 年江西省臭氧污染特征与气象因子影响分析 钱悦, 许彬, 夏玲君, 陈燕玲, 邓力琛, 王欢, 张根 (2190)

天山北坡城市群气溶胶光学特性时空分布特征 张喆, 丁建丽, 王瑾杰, 陈香月, 刘兴涛, 阿提干·吾斯曼 (2202)

基于高分影像的城市水体遥感综合分级方法 杨子谦, 刘怀庆, 吕恒, 李云梅, 朱利, 周亚明, 李玲玲, 毕顺 (2213)

太湖水体 Chl-a 预测模型 ARIMA 的构建及应用优化 李娜, 李勇, 冯家成, 单雅洁, 钱佳宁 (2223)

松花湖水水质空间差异及富营养化空间自相关分析 丁洋, 赵进勇, 张晶, 付意成, 彭文启, 陈渠昌, 李艳艳 (2232)

会仙岩溶湿地丰平枯水期地表水污染及灌溉适用性评价 朱丹尼, 邹胜章, 李军, 樊连杰, 赵一, 谢浩, 朱天龙, 潘民强, 徐利 (2240)

京杭大运河中下游段天然水化学变化特征及驱动因素 程中华, 邓义祥, 卓小可, 代丹, 于涛 (2251)

次降雨过程中不同土地利用配置对径流中氮流失的影响 罗义峰, 陈方鑫, 周豪, 龙翼, 严冬春, 谭文浩, 李丹丹, 陈晓燕 (2260)

碳氮同位素解析典型岩溶流域地下水中硝酸盐来源与归趋 任坤, 潘晓东, 梁嘉鹏, 彭聪, 曾洁 (2268)

冰封状态下达里湖冰-水中浮游细菌群落结构差异 李文宝, 杨旭, 田雅楠, 杜蕾 (2276)

城市再生水河道沉积物细菌群落空间变化分析:以京津冀北运河为例 邱莹, 靳燕, 苏振华, 邱琰若, 赵栋梁, 郭道宇 (2287)

太湖春夏两季反硝化与厌氧氨氧化速率的空间差异及其影响因素 赵锋, 许海, 詹旭, 朱广伟, 郭宇龙, 康丽娟, 朱梦圆 (2296)

三峡库区典型支流水库浮游动植物群落结构特征及其与环境因子的关系 陈莎, 谢青, 付梅, 江韬, 王永敏, 王定勇 (2303)

铁硫改性生物炭去除水中的磷 桑倩倩, 王芳君, 赵元添, 周强, 蔡雨麒, 邓颖, 田文清, 陈永志, 马娟 (2313)

钢渣对水体中磷的去除性能及机制解析 罗晓, 张峻搏, 何磊, 杨雪晶, 吕鹏翼 (2324)

BS-18 两性修饰膨润土对四环素和诺氟沙星复合污染的吸附 王新欣, 孟昭福, 刘欣, 王腾, 胡啸龙, 孙秀贤 (2334)

Ag₃PO₄/g-C₃N₄ 复合光催化剂的制备及其可见光催化性能 高闯闯, 刘海成, 孟无霜, 郝双玲, 薛婷婷, 陈国栋, Joseph Acquah (2343)

可见光驱动下罗丹明 B 自活化过硫酸盐降解双酚 A 张怡晨, 白雪, 石娟, 金鹏康 (2353)

铁钛共掺杂氧化铝诱发表面双反应中心催化臭氧氧化去除水中污染物 张帆, 宋阳, 胡春, 吕来 (2360)

硫化铁铜双金属复合材料的制备及除铬机制 屈敏, 王源, 陈辉霞, 王兴润, 徐红彬 (2370)

电催化-生物电化学耦合系统处理青霉素废水的机制 曲有鹏, 吕江维, 董跃, 冯玉杰, 张杰 (2378)

缺氧/好氧交替连续流的生活污水好氧颗粒污泥运行及污染物去除机制 李冬, 杨敬畏, 李悦, 李帅, 张诗睿, 王文强, 张杰 (2385)

反硝化除磷污泥聚集体内原位除磷活性及有机物浓度的影响 吕永涛, 姜晓童, 徒彦, 王旭东, 潘永宝, 刘爽, 崔双科, 王磊 (2396)

基于臭氧旁路处理的污泥原位减量技术工艺 薛冰, 刘宾寒, 韦婷婷, 王先恺, 陈思思, 董滨 (2402)

活性炭对城市有机固废厌氧消化过程抗生素抗性基因行为特征的影响 马佳莹, 王盼亮, 汪冰寒, 苏应龙, 谢冰 (2413)

6 种农业废弃物初期碳源及溶解性有机物释放机制 凌宇, 闫国凯, 王海燕, 董伟羊, 王欢, 常洋, 李丛宇 (2422)

中国典型农田土壤有机碳密度的空间分异及影响因素 李成, 王让会, 李兆哲, 徐扬 (2432)

不同水分条件和微生物生物量水平下水稻土有机碳矿化及其影响因子特征 刘琪, 李宇虹, 李哲, 魏晓梦, 祝贞科, 吴金水, 葛体达 (2440)

青藏高原林地土壤的氮转化特征及其影响因素分析:以祁连山和藏东南地区为例 何芳, 张丽梅, 申聪聪, 陈金全, 刘四义 (2449)

基于物元可拓模型的兰州市主城区公园表土重金属污染评价 胡梦瑶, 李春艳, 李娜娜, 吉天琪, 郑登友 (2457)

长期施用化肥和有有机肥对稻田土壤重金属及其有效性的影响 夏文建, 张丽芳, 刘增兵, 张文学, 蓝贤瑾, 刘秀梅, 刘佳, 刘光荣, 李祖章, 王萍 (2469)

川南山区土壤与农作物重金属特征及成因 韩伟, 王成文, 彭敏, 王乔林, 杨帆, 徐仁廷 (2480)

宁东能源化工基地核心区表层土壤中多环芳烃的空间分布特征、源解析及风险评价 杨帆, 罗红雪, 钟艳霞, 王幼奇, 白一茹 (2490)

重金属钝化剂阻控生菜 Cd 吸收的功能稳定性和适用性 鹿发虎, 吴雪姣, 孔雪菲, 曾亮, 王晓宇, 陈兆进, 姚伦广, 韩辉 (2502)

典型污染稻田水分管理对水稻镉累积的影响 张雨婷, 田应兵, 黄道友, 张泉, 许超, 朱挥华, 朱奇宏 (2512)

油茶果壳改性生物炭吸附性能及其耦合淹水对土壤 Cd 形态影响 蔡彤, 杜辉辉, 刘孝利, 铁柏清, 杨宇 (2522)

土地利用变化对松花江下游湿地土壤真菌群落结构及功能的影响 徐飞, 张拓, 怀宝东, 隋文志, 杨雪 (2531)

渔业复垦塌陷地抗生素抗性基因与微生物群落 程森, 路平, 冯启言 (2541)

3 种常用除草剂对细菌抗生素耐药性的影响 李曦, 廖汉鹏, 崔鹏, 白玉丹, 刘晨, 文畅, 周顺桂 (2550)

污水再生利用微生物控制标准及其制定方法探讨 陈卓, 崔琦, 曹可凡, 陆韻, 巫寅虎, 胡洪营 (2558)

《环境科学》征订启事 (2439) 《环境科学》征稿简则 (2479) 信息 (2152, 2231, 2286)

反硝化除磷污泥聚集体内原位除磷活性及有机物浓度的影响

吕永涛^{1,2}, 姜晓童^{1,2}, 徒彦^{1,2}, 王旭东^{1,2}, 潘永宝³, 刘爽³, 崔双科³, 王磊^{1,2*}

(1. 西安建筑科技大学环境与市政工程学院, 西安 710055; 2. 陕西省膜分离技术研究院陕西省膜分离重点实验室, 西安 710055; 3. 陕西省现代建筑设计研究院, 西安 710024)

摘要:以 SBR 系统反硝化除磷污泥为对象, 利用氧化还原电位、溶解氧和磷酸盐微电极定量研究了污泥聚集体内除磷菌的原位除磷活性及有机物浓度的影响。结果发现, 厌氧初期污泥聚集体内最大净体积释磷速率为 $3.29 \text{ mg} \cdot (\text{cm}^3 \cdot \text{h})^{-1}$, 是缺氧初期最大净体积吸磷速率的 3 倍左右; 厌氧末期释磷速率明显降低, 最大净体积释磷速率仅为厌氧初期的一半。在缺氧末期, 最大净体积吸磷速率降至 $0.14 \text{ mg} \cdot (\text{cm}^3 \cdot \text{h})^{-1}$, 且在 $1800 \mu\text{m}$ 以下深层区域发生了“二次释磷”现象。随着 COD 浓度由 $350 \text{ mg} \cdot \text{L}^{-1}$ 降至 $250 \text{ mg} \cdot \text{L}^{-1}$ 和 $150 \text{ mg} \cdot \text{L}^{-1}$, 反硝化除磷菌的最大净体积释磷速率由 $3.27 \text{ mg} \cdot (\text{cm}^3 \cdot \text{h})^{-1}$ 降至 $2.44 \text{ mg} \cdot (\text{cm}^3 \cdot \text{h})^{-1}$ 和 $2.01 \text{ mg} \cdot (\text{cm}^3 \cdot \text{h})^{-1}$, 且快速吸磷区域整体向污泥聚集体表层收窄。

关键词:反硝化除磷; 微电极; 污泥聚集体; 净体积速率; 有机物浓度

中图分类号: X703 文献标识码: A 文章编号: 0250-3301(2021)05-2396-06 DOI: 10.13227/j.hjks.202010109

In-situ Phosphorus Removal Activity and Impact of the Organic Matter Concentration on Denitrifying Phosphorus Removal in Sludge Aggregates

LÜ Yong-tao^{1,2}, JIANG Xiao-tong^{1,2}, TU Yan^{1,2}, WANG Xu-dong^{1,2}, PAN Yong-bao³, LIU Shuang³, CUI Shuang-ke³, WANG Lei^{1,2*}

(1. School of Environmental and Municipal Engineering, Xi'an University of Architecture and Technology, Xi'an 710055, China; 2. Key Laboratory of Membrane Separation of Shaanxi Province, Research Institute of Membrane Separation Technology of Shaanxi Province, Xi'an 710055, China; 3. Shaanxi Modern Architecture Design & Research Institute, Xi'an 710024, China)

Abstract: In this work, the redox potential, dissolved oxygen, and phosphate microelectrodes were used to quantitatively study the in-situ activity of dephosphorization bacteria and the impact of the organic matter concentration on denitrifying phosphorus removal in sludge aggregates in a sequencing batch reactor. The results showed that the maximum net volume release rate of phosphorus was $3.29 \text{ mg} \cdot (\text{cm}^3 \cdot \text{h})^{-1}$ in the initial anaerobic sludge aggregates, which was approximately 3 times the maximum net volume uptake rate of phosphorus at the initial anoxic stage. The release rate of phosphorus clearly decreased at the final anaerobic stage, and the maximum net volume release rate of phosphorus was only half of that at the initial anaerobic stage. At the final anoxic stage, the maximum net volume uptake rate of phosphorus decreased to $0.14 \text{ mg} \cdot (\text{cm}^3 \cdot \text{h})^{-1}$, and the phenomenon of secondary phosphorus release occurred in the deep area below $1800 \mu\text{m}$. When the concentration of COD decreased from $350 \text{ mg} \cdot \text{L}^{-1}$ to $250 \text{ mg} \cdot \text{L}^{-1}$ and $150 \text{ mg} \cdot \text{L}^{-1}$, the maximum net volume release rate of phosphorus of dephosphorization bacteria decreased from $3.27 \text{ mg} \cdot (\text{cm}^3 \cdot \text{h})^{-1}$ to $2.44 \text{ mg} \cdot (\text{cm}^3 \cdot \text{h})^{-1}$ and $2.01 \text{ mg} \cdot (\text{cm}^3 \cdot \text{h})^{-1}$, respectively, and the rapid uptake area of phosphorus narrowed to the surface of the sludge aggregates.

Key words: denitrifying phosphorus removal; microelectrode; sludge aggregates; net volume rate; organic matter concentration

反硝化除磷是指在缺氧条件利用 NO_x^- 氧化胞内聚合物, 同时完成反硝化脱氮和除磷的生物过程^[1,2]. 因可“一碳两用”, 具有节省碳源、降低曝气量和污泥产量^[3~9]的优点, 成为本领域的研究热点之一. 研究者通过试验研究获得了反硝化除磷的影响因素及运行参数^[10~15], 但大部分停留在反应器去除效能等宏观层面.

微生物活性是反应器去除效能的决定因素, 有研究者利用尖端细小的微电极测定污泥基因(污泥聚集体或生物膜等)内部物质浓度的空间分布特征, 获得了原位生物活性, 从而为污水处理问题诊断或优化提供依据^[16]. 目前, 研究对象多针对脱氮系

统^[17~21], 对除磷污泥聚集体原位生物活性的研究尚少见报道. Lee 等^[22]利用磷酸盐微电极, 测定了厌氧条件下污泥内的磷浓度的空间分布特性, 首次揭示了除磷菌的原位生物活性. 吕永涛等^[23]研究获得了污水厂 A²/O 工艺沿程处理单元除磷菌活性的变化规律, 为污水处理参数的优化提供了一定依据.

本文在 SBR 系统中实现了反硝化除磷的启动

收稿日期: 2020-10-19; 修订日期: 2020-11-09

基金项目: 陕西省重点研发计划项目(2020SF-415); 陕西省重点科技创新团队计划项目(2017KCT-19-01); 陕西省技术创新引导专项(2018HJCG-18)

作者简介: 吕永涛(1980~), 男, 博士, 副教授, 主要研究方向为污水处理与资源化, E-mail: hybos2000@126.com

* 通信作者, E-mail: wl0178@126.com

与稳定运行.在此基础上,利用微电极定量研究了厌氧和缺氧段污泥聚集体内的原位除磷生物活性以及有机物浓度对释磷活性的影响,通过揭示反硝化除磷的原位生物活性,以期系统的优化提供一定的依据.

1 材料与方法

1.1 试验装置

采用圆柱形 SBR 反应器,内径 15 cm,高 34 cm,有效容积 5 L,排水比为 0.6.采用磁力搅拌器使泥水混合均匀,通过 PLC 自动控制反应器的连续运行.

1.2 运行操作

反应器每天运行 3 个周期,单周期运行时间为 8 h,具体包括:厌氧进水(3 L)5 min,厌氧搅拌 164 min,沉淀排水(3 L)47 min,缺氧进水(3 L)5 min,缺氧搅拌 216 min,沉淀排水(3 L)47 min.

1.3 接种污泥与试验用水

反应器所用污泥取自西安某污水处理厂,接种后初始污泥浓度约为 $4\ 000\ \text{mg}\cdot\text{L}^{-1}$,稳定运行期间控制 SRT 为 15 d,污泥浓度维持在 $(3\ 700 \pm 200)\ \text{mg}\cdot\text{L}^{-1}$,SVI 约为 $52.5\ \text{mL}\cdot\text{g}^{-1}$.

进水基质人工配置,厌氧段主要为乙酸钠和 NaHCO_3 ,其中 COD $200 \sim 330\ \text{mg}\cdot\text{L}^{-1}$, $\text{NH}_4^+\text{-N}$ $10 \sim 30\ \text{mg}\cdot\text{L}^{-1}$, NaHCO_3 $200\ \text{mg}\cdot\text{L}^{-1}$.缺氧段主要为 KH_2PO_4 、 KNO_3 和 NaHCO_3 ,其中 $\text{NO}_3^-\text{-N}$ $19.9 \sim 58\ \text{mg}\cdot\text{L}^{-1}$, $\text{PO}_4^{3-}\text{-P}$ $19 \sim 26\ \text{mg}\cdot\text{L}^{-1}$, NaHCO_3 $200\ \text{mg}\cdot\text{L}^{-1}$.另外,每升进水中加入 1 mL 的微量元素,成分按文献[24]配制.

1.4 化学分析方法

按文献[25]的方法进行测定,其中,氨氮采用纳氏试剂分光光度法,化学需氧量采用重铬酸钾法,亚硝氮采用 *N*-(1-萘基)-乙二胺比色法,硝氮采用盐酸-氨基磺酸比色法,磷酸盐采用钼酸盐分光光度法,溶解氧采用哈希便携式溶氧仪.

1.5 微电极系统与测试方案

1.5.1 微电极及性能

采用氧化还原电位、溶解氧和磷酸盐微电极均为课题组自制.其中,氧化还原电位、溶解氧微电极尖端直径小于 $25\ \mu\text{m}$,响应时间在 65 s 内,标准曲线的 $R^2 = 0.995 \pm 0.002$.磷酸盐微电极尖端直径约为 $20\ \mu\text{m}$,标准曲线的 $R^2 > 0.992$,响应时间小于 90 s.

1.5.2 微电极测试装置与方法

采用升流式测试槽^[18],通过开启蠕动泵将厚度约为 $5\ 000\ \mu\text{m}$ 的污泥悬浮在丝状网上^[26,27].30 min 后,待传质稳定后开始测量.由于污泥层中的物质浓

度呈对称分布,所以本试验测定 $0 \sim 2\ 500\ \mu\text{m}$ 的上层深度.

1.5.3 试验方案

(1)反硝化除磷污泥聚集体的原位生物活性分别在厌氧初期(反应初始 1 min)、厌氧末期(反应最后 1 min)、缺氧初期(反应初始 1 min)、缺氧末期(反应最后 1 min)各取 100 mL 泥水混合液,放置在微电极测试槽里,使污泥悬浮在丝状网上,30 min 后开始测定环境及物质的空间浓度.

(2)COD 浓度对厌氧释磷原位活性影响 厌氧反应初始 1 min 取泥水混合液 100 mL,完成泥水分离后置于丝状网上,测试槽中分别配置 COD 为 150、250 和 $350\ \text{mg}\cdot\text{L}^{-1}$ 的基质进行微电极测试.

每个样品利用每种微电极分别测量 3 次,试验结果取 3 次试验平均值.

1.6 净体积产生/消耗速率计算

根据污泥聚集体内 $\text{PO}_4^{3-}\text{-P}$ 的空间浓度,利用 Fick 第二定律,计算除磷菌的净体积产生/消耗速率^[28,29].其中,负值表示产生速率,正值表示消耗速率.

2 结果与讨论

2.1 SBR 系统反硝化除磷的启动与运行性能

通过逐步提升进水 COD、 PO_4^{3-} 及 NO_3^- 的浓度,实现了反硝化除磷的启动,具体见图 1.从中可见,随着驯化时间的增长,除磷效率逐渐增加.第 1 d,除磷量为 $2.70\ \text{mg}\cdot\text{L}^{-1}$,表明接种污泥中存在一定的反硝化聚磷菌.第 2 ~ 10 d,除磷量由 $1.90\ \text{mg}\cdot\text{L}^{-1}$ 增至 $8.63\ \text{mg}\cdot\text{L}^{-1}$;之后,逐渐升至 $14.91\ \text{mg}\cdot\text{L}^{-1}$,并趋于稳定,反应器具备较高的除磷能力.

NO_3^- 的去除几乎与除磷效果同步变化,前 10 d, NO_3^- -N 进水浓度为 $20 \sim 26\ \text{mg}\cdot\text{L}^{-1}$,出水 NO_3^- -N

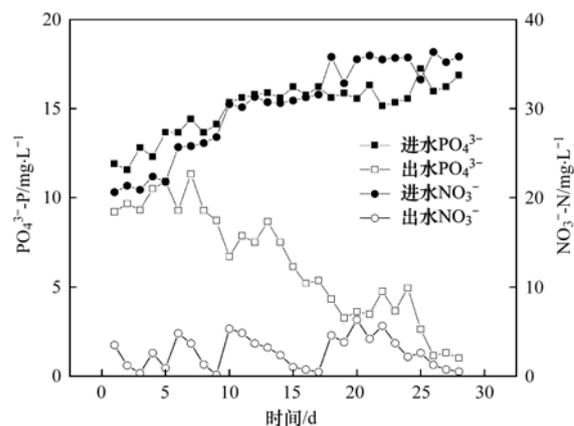


图 1 启动阶段 SBR 反应器缺氧段吸磷和 NO_3^- -N 去除率变化情况
Fig. 1 Changes in phosphorus uptake and the NO_3^- -N removal rate in the anoxic stage of the SBR reactor during the start-up phase

浓度在 $0.16 \sim 4.82 \text{ mg}\cdot\text{L}^{-1}$ 间波动. 为进一步满足除磷所需电子供体, 第 10 d 至 15 d, 进水 $\text{NO}_3^- \text{-N}$ 浓度提高至 $30 \text{ mg}\cdot\text{L}^{-1}$, 去除率由 82.52% 逐渐提高至 92.23%; 第 18 d 起, $\text{NO}_3^- \text{-N}$ 浓度升至 $35 \text{ mg}\cdot\text{L}^{-1}$, 去除率逐渐稳定在 97.00% 以上, 获得了稳定的反硝化除磷效果.

2.2 反硝化除磷污泥聚集体内原位除磷活性

2.2.1 厌氧段污泥聚集体内释磷的原位生物活性

厌氧段污泥聚集体内释磷原位生物活性的变化规律见图 2. 由图 2(a) 可见, 厌氧初始 1 min, DO 和 ORP 随深度增加均呈降低的趋势, 其中, DO 由 $0.28 \text{ mg}\cdot\text{L}^{-1}$ 降至 $0.05 \text{ mg}\cdot\text{L}^{-1}$, ORP 由 -67.58 mV 降至 -128.41 mV , 可知污泥聚集体内为厌氧环境. $\text{PO}_4^{3-} \text{-P}$ 浓度呈逐渐升高的趋势, 最大值为 $47.18 \text{ mg}\cdot\text{L}^{-1}$. 经计算, 其最大释磷速率发生在表层 $500 \mu\text{m}$ 左右, 达到 $3.30 \text{ mg}\cdot(\text{cm}^3\cdot\text{h})^{-1}$.

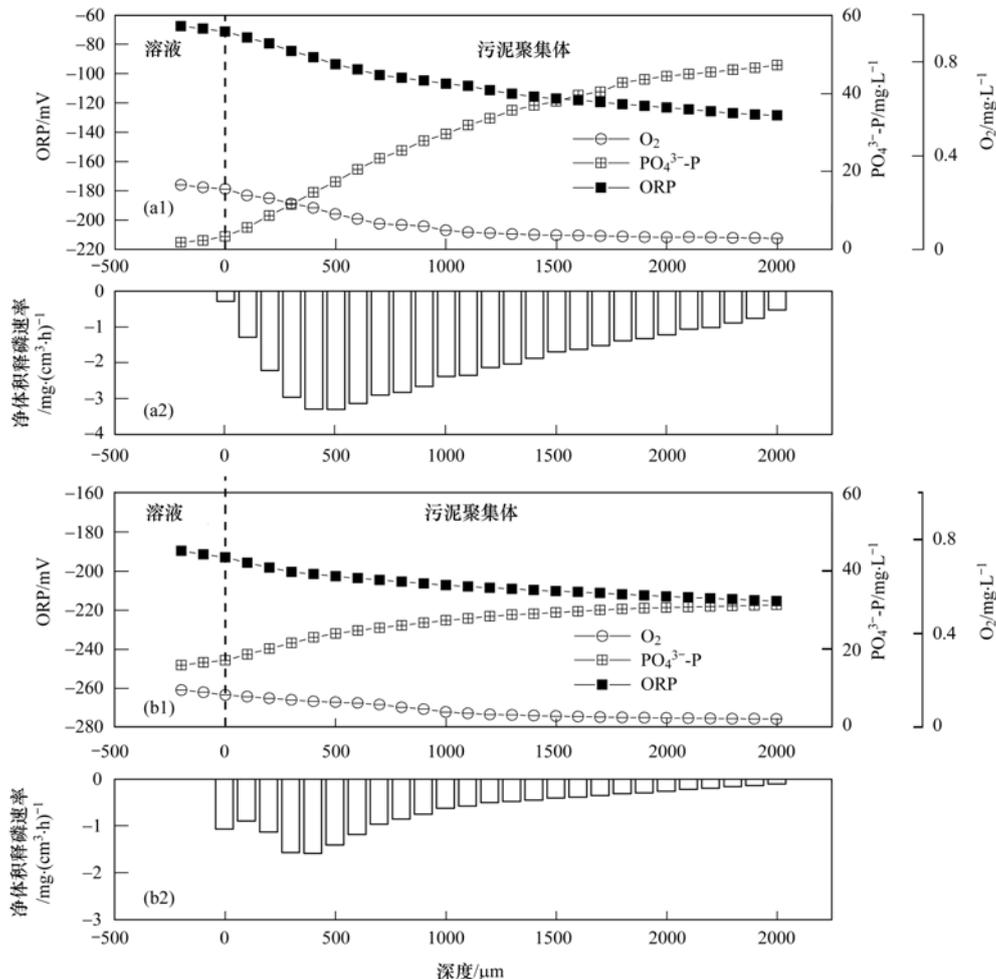
由图 2(b) 可见, 厌氧末期 1 min, DO 与 ORP 的变化趋势同厌氧初期, ORP 最低降至 -215.46 mV , 表明随着反应进行, 反应器 ORP 进一步降低;

$\text{PO}_4^{3-} \text{-P}$ 浓度由 $15.88 \text{ mg}\cdot\text{L}^{-1}$ 升至 $31.32 \text{ mg}\cdot\text{L}^{-1}$, 最大净体积释磷速率发生在表层 $400 \mu\text{m}$ 处, 为 $1.60 \text{ mg}\cdot(\text{cm}^3\cdot\text{h})^{-1}$.

综上所述, 相比于厌氧初期, 末期的最大净体积释磷速率大大减小, 仅为初期的一半左右. 污泥深层区域 ($>1000 \mu\text{m}$), 厌氧末期的释磷反应基本停止. 此外, 最大净体积释磷速率均发生在表层 $400 \sim 500 \mu\text{m}$ 处, 此处的 ORP 分别为 -93.62 mV (初期) 和 -201.63 mV (末期), 说明, 碳源充足条件下, 只要 ORP 低于 -93.62 mV 均可获得最高释磷速率. 与宏观试验发现 ORP 能指示厌氧释磷的结果相一致^[17,18]. 另外, 当污泥聚集体内(生物膜或颗粒污泥)厚度超过 $500 \mu\text{m}$, 可能会因传质受限影响释磷速率.

2.2.2 缺氧段污泥聚集体内吸磷的原位生物活性

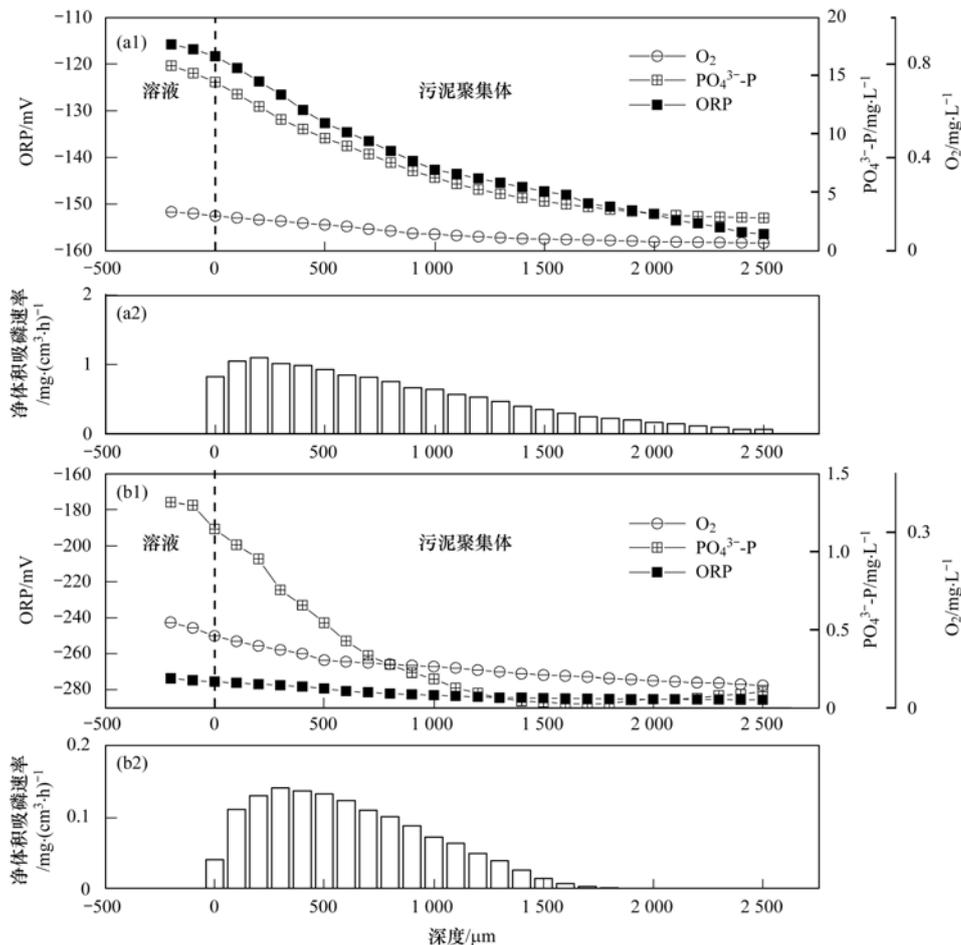
缺氧段污泥聚集体内吸磷速率, 结果见图 3. 由图 3(a) 可见, 缺氧初始 1 min, 污泥聚集体内 DO 浓度变化不大, 由 $0.17 \text{ mg}\cdot\text{L}^{-1}$ 降至 $0.03 \text{ mg}\cdot\text{L}^{-1}$; ORP 迅速降低, 由表层的 -115.76 mV 降至



(a) 厌氧初始 1 min; (b) 厌氧末期 1 min

图 2 厌氧段污泥聚集体内浓度空间分布及净体积释磷速率

Fig. 2 Spatial distribution of the concentration and net volume release rate of $\text{PO}_4^{3-} \text{-P}$ in the anaerobic sludge aggregates



(a) 缺氧初始 1 min; (b) 缺氧末期 1 min

图3 缺氧段污泥聚集体内浓度分布及吸磷净体积速率

Fig. 3 Spatial distribution of the concentration and net volume uptake rate of $\text{PO}_4^{3-}\text{-P}$ in the anoxic period sludge aggregates

-156.46 mV; $\text{PO}_4^{3-}\text{-P}$ 浓度呈下降趋势,由 $15.88 \text{ mg}\cdot\text{L}^{-1}$ 降至 $2.80 \text{ mg}\cdot\text{L}^{-1}$. 经计算,最大净体积吸磷速率发生在 $200 \mu\text{m}$ 处,为 $1.10 \text{ mg}\cdot(\text{cm}^3\cdot\text{h})^{-1}$.

由图3(b)可见,缺氧末期 1 min, DO 浓度分布与初期几乎一样; ORP 较初期更低,由 -273.68 mV 降至 -285.49 mV , $\text{PO}_4^{3-}\text{-P}$ 浓度呈减小的趋势,从污泥表层的 $1.32 \text{ mg}\cdot\text{L}^{-1}$ 降至 $0.10 \text{ mg}\cdot\text{L}^{-1}$. 经计算,最大净体积吸磷速率发生在表层 $300 \mu\text{m}$, 仅为 $0.14 \text{ mg}\cdot(\text{cm}^3\cdot\text{h})^{-1}$. 此外,在 $1800 \mu\text{m}$ 以下的深层区域, $\text{PO}_4^{3-}\text{-P}$ 浓度略有上升,发生轻微的释磷现象.

综上,污泥聚集体内反硝化吸磷的最大净体积速率为 $1.10 \text{ mg}\cdot(\text{cm}^3\cdot\text{h})^{-1}$, 仅为最大释磷速率的 $1/3$ 左右. 因此,缺氧段需要更多的反应时间. 缺氧末期吸磷反应很微弱,且在污泥聚集体深处发生了“二次释磷”现象,与宏观研究结果相一致^[22]. 笔者推测可能是由于缺氧末期电子受体 NO_3^- 不足发生了内源释磷. 因此,为保证除磷效果反应器应严格控

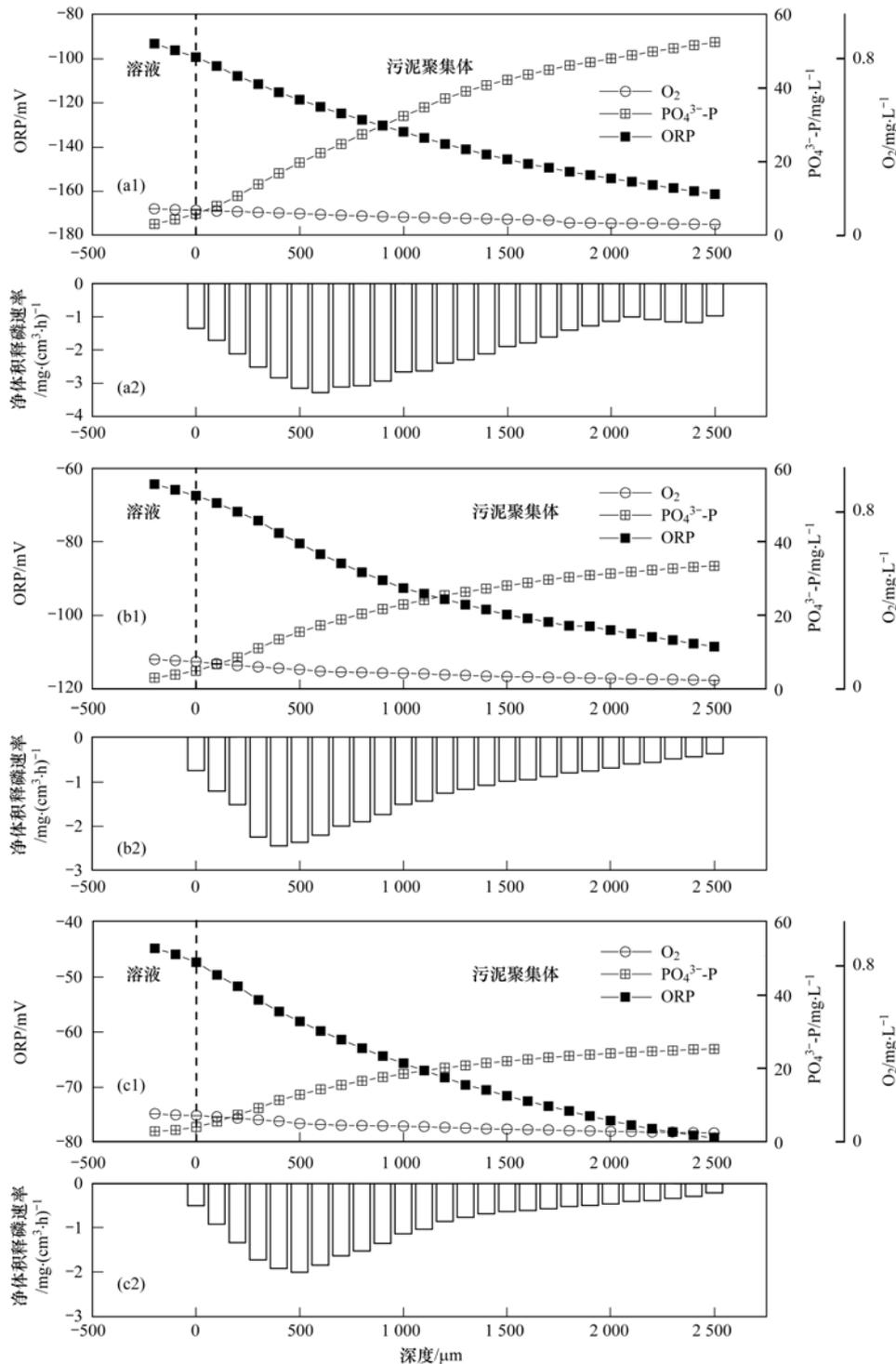
制缺氧段的运行时间.

2.3 COD 浓度对污泥聚集体内原位释磷活性的影响

在厌氧初始 1 min 取样,研究不同 COD 浓度对污泥聚集体内原位释磷活性的影响,结果见图 4. 从中可知,3 组试验中 DO 变化值较小,均为 $0.07 \sim 0.09 \text{ mg}\cdot\text{L}^{-1}$. 随着 COD 浓度 ($\text{mg}\cdot\text{L}^{-1}$) 由 350 降至 250 和 150, ORP 在整个污泥聚集体中的变化值呈降低趋势,分别为 68.00 、 44.07 和 34.56 mV , 最大释磷净体积速率分别由 $3.27 \text{ mg}\cdot(\text{cm}^3\cdot\text{h})^{-1}$ 降至 $2.44 \text{ mg}\cdot(\text{cm}^3\cdot\text{h})^{-1}$ 和 $2.01 \text{ mg}\cdot(\text{cm}^3\cdot\text{h})^{-1}$. 表明高浓度的 COD, 同时降低了 ORP 并提高了释磷速率. 此外,随着初始 COD 浓度的降低,快速释磷区域向污泥聚集体的表层收窄,原因是低 COD 浓度导致传质减弱,使污泥整体释磷活性降低.

3 结论

(1) 反硝化除磷污泥聚集体内部,原位释磷活性远高于吸磷活性,最大释磷速率是吸磷速率的



(a) COD 浓度为 $350 \text{ mg}\cdot\text{L}^{-1}$; (b) COD 浓度为 $250 \text{ mg}\cdot\text{L}^{-1}$; (c) COD 浓度为 $150 \text{ mg}\cdot\text{L}^{-1}$

图 4 COD 浓度对污泥聚集体内浓度分布及净体积释磷速率的影响

Fig. 4 Effect of the COD concentration on the concentration distribution in the sludge aggregates and the net volume release rate of $\text{PO}_4^{3-}\text{-P}$

3 倍.

(2) 厌氧和缺氧段末期, 虽然污泥聚集体内的 ORP 均进一步降低, 但因浓度降低导致基质受限, 其释磷、吸磷速率仅为初期的 1/2 和 1/8 左右.

(3) 随着 COD 浓度的降低, 反硝化除磷污泥聚集体内净体积释磷速率呈降低趋势, 且快速释磷区域向表层收窄.

参考文献:

- [1] Tian W D, Ma C, Lin Y, *et al.* Effect of Mg/Ca molar ratios on characteristics of anaerobic-anoxic denitrifying dephosphatation [J]. *Bioresource Technology*, 2017, **240**: 94-97.
- [2] Dai H L, Wu Y F, Peng L H, *et al.* Effects of calcium on the performance, bacterial population and microbial metabolism of a denitrifying phosphorus removal system [J]. *Bioresource Technology*, 2017, **243**: 828-835.
- [3] Lee J K, Choi C K, Lee K H, *et al.* Mass balance of nitrogen,

- and estimates of COD, nitrogen and phosphorus used in microbial synthesis as a function of sludge retention time in a sequencing batch reactor system [J]. *Bioresource Technology*, 2008, **99** (16): 7788-7796.
- [4] Wang J L, Peng Y Z, Wang S Y, *et al.* Nitrogen removal by simultaneous nitrification and denitrification *via* nitrite in a sequence hybrid biological reactor [J]. *Chinese Journal of Chemical Engineering*, 2008, **16**(5): 778-784.
- [5] Bortone G, Libelli S M, Tilche A, *et al.* Anoxic phosphate uptake in the dephano process [J]. *Water Science and Technology*, 1999, **40**(4-5): 177-185.
- [6] 王亚宜, 彭永臻, 王淑莹, 等. 反硝化除磷理论、工艺及影响因素[J]. *中国给水排水*, 2003, **19**(1): 33-36.
Wang Y Y, Peng Y Z, Wang S Y, *et al.* Denitrifying phosphorus removal theory, technology and the affecting factors [J]. *China Water & Wastewater*, 2003, **19**(1): 33-36.
- [7] 王晓霞, 王淑莹, 赵曦, 等. SPNED-PR 系统内 PAOs-GAOs 的竞争关系及其氮磷去除特性[J]. *中国环境科学*, 2018, **38**(2): 551-559.
Wang X X, Wang S Y, Zhao J, *et al.* The competitive relationships of PAOs-GAOs in simultaneous partial nitrification-endogenous denitrification and phosphorous removal (SPNED-PR) systems and their nutrient removal characteristics [J]. *China Environmental Science*, 2018, **38**(2): 551-559.
- [8] 韦佳敏, 蒋志云, 程诚, 等. ABR-MBR 反硝化除磷工艺的启动及稳定运行[J]. *环境科学*, 2019, **40**(2): 808-815.
Wei J M, Jiang Z Y, Cheng C, *et al.* Start-up and stable operation of ABR-MBR denitrifying phosphorus removal process [J]. *Environmental Science*, 2019, **40**(2): 808-815.
- [9] 李伟光, 李东辉, 姚杰, 等. 污泥龄对 BBSNP 工艺反硝化除磷脱氮效能的影响[J]. *中国给水排水*, 2020, **36**(17): 13-17.
Li W G, Li D H, Yao J, *et al.* Effect of sludge retention time on nitrogen and phosphorus removal Efficiency of bi-bio-selector for nitrogen and phosphorus removal process [J]. *China Water Wastewater*, 2020, **36**(17): 13-17.
- [10] 缪新年, 汪倩, 郭凯成, 等. ABR-MBR 耦合工艺启动及优化反硝化除磷性能[J]. *环境科学*, 2020, **41**(9): 4150-4160.
Miao X N, Wang Q, Guo K C, *et al.* Start-up and optimization of denitrifying phosphorus removal in ABR-MBR coupling process [J]. *Environmental Science*, 2020, **41**(9): 4150-4160.
- [11] Dulekgurgen E, Ovez S, Artan N, *et al.* Enhanced biological phosphate removal by granular sludge in a sequencing batch reactor [J]. *Biotechnology Letters*, 2003, **25**(9): 687-693.
- [12] 赵凯亮, 刘安迪, 南彦斌, 等. HRT 对改良式 A²/O-BAF 反硝化除磷脱氮的影响[J]. *环境科学*, 2020, **41**(6): 2771-2778.
Zhao K L, Liu A D, Nan Y B, *et al.* Effect of HRT on denitrifying phosphorus and nitrogen removal in modified A²/O-BAF [J]. *Environmental Science*, 2020, **41**(6): 2771-2778.
- [13] Azhdarpoor A, Mohammadi P, Dehghani M. Simultaneous removal of nutrients in a novel anaerobic-anoxic/aerobic sequencing reactor; removal of nutrients in a novel reactor [J]. *International Journal of Environmental Science and Technology*, 2016, **13**(2): 543-550.
- [14] Kumar S, Quaff A R. Treatment of domestic wastewater containing phosphate using water treatment sludge through UASB-clariflocculator integrated system [J]. *Environment, Development and Sustainability*, 2020, **22**(5): 4537-4550.
- [15] 韦佳敏, 黄慧敏, 程诚, 等. 污泥龄及 pH 值对反硝化除磷工艺效能的影响[J]. *环境科学*, 2019, **40**(4): 1900-1905.
Wei J M, Huang H M, Cheng C, *et al.* Effect of sludge retention time and pH on the denitrifying phosphorus removal process [J]. *Environmental Science*, 2019, **40**(4): 1900-1905.
- [16] Li B K, Bishop P L. Micro-profiles of activated sludge floc determined using microelectrodes [J]. *Water Research*, 2004, **38**(5): 1248-1258.
- [17] Lv Y T, Ju K, Wang L, *et al.* Effect of pH on nitrous oxide production and emissions from a partial nitrification reactor under oxygen-limited conditions [J]. *Process Biochemistry*, 2016, **51** (6): 765-771.
- [18] Lv Y T, Ju K, Sun T, *et al.* Effect of the dissolved oxygen concentration on the N₂O emission from an autotrophic partial nitrification reactor treating high-ammonium wastewater [J]. *International Biodeterioration & Biodegradation*, 2016, **114**: 209-215.
- [19] Kinh C T, Suenaga T, Hori T, *et al.* Counter-diffusion biofilms have lower N₂O emissions than co-diffusion biofilms during simultaneous nitrification and denitrification; insights from depth-profile analysis [J]. *Water Research*, 2017, **124**: 363-371.
- [20] Zhou X, Zhang Z Q, Zhang X N, *et al.* A novel single-stage process integrating simultaneous COD oxidation, partial nitrification-denitrification and anammox (SCONDA) for treating ammonia-rich organic wastewater [J]. *Bioresource Technology*, 2018, **254**: 50-55.
- [21] Cao Y F, Zhang C S, Rong H W, *et al.* The effect of dissolved oxygen concentration (DO) on oxygen diffusion and bacterial community structure in moving bed sequencing batch reactor (MBSBR) [J]. *Water Research*, 2017, **108**: 86-94.
- [22] Lee W H, Seo Y, Bishop P L. Characteristics of a cobalt-based phosphate microelectrode for *in situ* monitoring of phosphate and its biological application [J]. *Sensors and Actuators B: Chemical*, 2009, **137**(1): 121-128.
- [23] 吕永涛, 徒彦, 吴浩伟, 等. A²/O 工艺中污泥聚集体内部除磷菌的原位活性研究[J]. *中国给水排水*, 2019, **35**(17): 31-36, 55.
Lü Y T, Tu Y, Wu H W, *et al.* In-situ activity of dephosphorization bacteria in sludge aggregates in A²/O process [J]. *China Water & Wastewater*, 2019, **35**(17): 31-36, 55.
- [24] Zhou Y, Pijuan M, Yuan Z G. Development of a 2-sludge, 3-stage system for nitrogen and phosphorous removal from nutrient-rich wastewater using granular sludge and biofilms [J]. *Water Research*, 2008, **42**(12): 3207-3217.
- [25] 国家环境保护总局. 水和废水监测分析方法 [M]. (第四版). 北京: 中国环境科学出版社, 2002. 258-284.
- [26] Lee W H, Bishop P L. In situ microscale analyses of activated sludge flocs in the enhanced biological phosphate removal process by the use of microelectrodes and fluorescent in situ hybridization [J]. *Journal of Environmental Engineering*, 2010, **136** (6): 561-567.
- [27] 王亚宜, 彭永臻, 王淑莹, 等. 碳源和硝态氮浓度对反硝化聚磷的影响及 ORP 的变化规律[J]. *环境科学*, 2004, **25** (4): 54-58.
Wang Y Y, Peng Y Z, Wang S Y, *et al.* Effect of carbon source and nitrate concentration on denitrifying dephosphorus removal and variation of ORP [J]. *Environmental Science*, 2004, **25** (4): 54-58.
- [28] Kim K S, Yoo J S, Kim S, *et al.* Relationship between the electric conductivity and phosphorus concentration variations in an enhanced biological nutrient removal process [J]. *Water Science & Technology*, 2007, **55**(1-2): 203-208.
- [29] 姜欣欣. A²SBR 反硝化除磷系统的试验研究 [D]. 哈尔滨: 哈尔滨工业大学, 2007. 7.
Jiang X X. Study on A²SBR denitrifying phosphorus removal system [D]. Harbin: Harbin Institute of Technology, 2007. 7.

CONTENTS

| | |
|---|--|
| Chemical Characteristics and Source Apportionment of Organic Aerosols in Atmospheric PM _{2.5} in Winter in Beijing | XU Nan, WANG Tian-tian, LI Xiao, <i>et al.</i> (2101) |
| Characteristics of Two Pollution Episodes Before and After City Heating in Beijing from February to March of 2019 | YIN Xiao-mei, PU Wei-wei, WANG Ji-kang, <i>et al.</i> (2110) |
| Analysis of Characteristics and Causes of a Typical Haze Pollution in Beijing in the Winter of 2019 | LIAN Han-yang, YANG Xin, ZHANG Pu, <i>et al.</i> (2121) |
| New Particle Formation Events in Summer and Winter in the Coastal Atmosphere in Qingdao, China | SUN Yue, ZHU Yu-jiao, MENG He, <i>et al.</i> (2133) |
| Characteristics of Heavy Metal Pollution and Ecological Risk Evaluation of Indoor Dust from Urban and Rural Areas in Taiyuan City During the Heating Season | HUANG Hao, XU Zi-qi, YAN Jun-xia, <i>et al.</i> (2143) |
| Concentration Analysis and Health Risk Assessment of Air Pollutants in Newly Decorated Public Places in Xi'an | FAN Jie, FAN Hao, SHEN Zhen-xing, <i>et al.</i> (2153) |
| Emission Concentration and Characteristics of Particulate Matter and Water-Soluble Ions in Exhaust Gas of Typical Combustion Sources with Ultra-Low Emission | HU Yue-qi, WANG Zheng, GUO Jian-hui, <i>et al.</i> (2159) |
| High-Throughput Sequencing Analysis of Microbial Communities in Summertime Atmospheric Particulate Matter in Hefei City | JIANG Shao-yi, SUN Bo-wen, DAI Hai-tao, <i>et al.</i> (2169) |
| Spatiotemporal Variations in Fine Particulate Matter and the Impact of Air Quality Control in Zhengzhou | DONG Zhe, YUAN Ming-hao, SU Fang-cheng, <i>et al.</i> (2179) |
| Characteristics of Ozone Pollution and Relationships with Meteorological Factors in Jiangxi Province | QIAN Yue, XU Bin, XIA Ling-jun, <i>et al.</i> (2190) |
| Temporal and Spatial Distribution Characteristics of Aerosol Optical Properties in Urban Agglomerations on the North Slope of the Tianshan Mountains | ZHANG Zhe, DING Jian-li, WANG Jin-jie, <i>et al.</i> (2202) |
| Comprehensive Classification Method of Urban Water by Remote Sensing Based on High-Resolution Images | YANG Zi-qian, LIU Huai-qing, LÜ Heng, <i>et al.</i> (2213) |
| Construction and Application Optimization of the Chl-a Forecast Model ARIMA for Lake Taihu | LI Na, LI Yong, FENG Jia-cheng, <i>et al.</i> (2223) |
| Spatial Differences in Water Quality and Spatial Autocorrelation Analysis of Eutrophication in Songhua Lake | DING Yang, ZHAO Jin-yong, ZHANG Jing, <i>et al.</i> (2232) |
| Pollution and Irrigation Applicability of Surface Water from Wet, Normal, and Dry Periods in the Huixian Karst Wetland, China | ZHU Dan-ni, ZOU Sheng-zhang, LI Jun, <i>et al.</i> (2240) |
| Changes in Water Chemistry and Driving Factors in the Middle and Lower Reaches of the Beijing-Hangzhou Grand Canal | CHENG Zhong-hua, DENG Yi-xiang, ZHUO Xiao-ke, <i>et al.</i> (2251) |
| Effects of Different Land Use Practices on Nitrogen Loss from Runoff During Rainfall Events | LUO Yi-feng, CHEN Fang-xin, ZHOU Hao, <i>et al.</i> (2260) |
| Sources and Fate of Nitrate in Groundwater in a Typical Karst Basin: Insights from Carbon, Nitrogen, and Oxygen Isotopes | REN Kun, PAN Xiao-dong, LIANG Jia-peng, <i>et al.</i> (2268) |
| Changes in the Bacterioplankton Community Between "Ice" and "Water" in the Frozen Dali Lake | LI Wen-bao, YANG Xu, TIAN Ya-nan, <i>et al.</i> (2276) |
| Analysis of the Spatial Changes in Bacterial Communities in Urban Reclaimed Water Channel Sediments; A Case Study of the North Canal River | QIU Ying, JIN Yan, SU Zhen-hua, <i>et al.</i> (2287) |
| Spatial Differences and Influencing Factors of Denitrification and ANAMMOX Rates in Spring and Summer in Lake Taihu | ZHAO Feng, XU Hai, ZHAN Xu, <i>et al.</i> (2296) |
| Structural Characteristics of Zooplankton and Phytoplankton Communities and Its Relationship with Environmental Factors in a Typical Tributary Reservoir in the Three Gorges Reservoir Region | CHEN Sha, XIE Qing, FU Mei, <i>et al.</i> (2303) |
| Application of Iron and Sulfate-Modified Biochar in Phosphorus Removal from Water | SANG Qian-qian, WANG Fang-jun, ZHAO Yuan-tian, <i>et al.</i> (2313) |
| Analysis of the Performance and Mechanism of Phosphorus Removal in Water by Steel Slag | LUO Xiao, ZHANG Jun-bo, HE Lei, <i>et al.</i> (2324) |
| Adsorption of BS-18 Amphoterically Modified Bentonite to Tetracycline and Norfloxacin Combined Pollutants | WANG Xin-xin, MENG Zhao-fu, LIU Xin, <i>et al.</i> (2334) |
| Preparation of Ag ₃ PO ₄ /g-C ₃ N ₄ Composite Photocatalysts and Their Visible Light Photocatalytic Performance | GAO Chuang-chuang, LIU Hai-cheng, MENG Wu-shuang, <i>et al.</i> (2343) |
| Activation of Permonosulfate by Rhodamine B for BPA Degradation Under Visible Light Irradiation | ZHANG Yi-chen, BAI Xue, SHI Juan, <i>et al.</i> (2353) |
| Fe-Ti Co-Doped Alumina-Induced Surface Dual Reaction Center for Catalytic Ozonation to Remove Pollutants from Water | ZHANG Fan, SONG Yang, HU Chun, <i>et al.</i> (2360) |
| Preparation of Sulfidated Copper-Iron Bimetallic Compositing Material and Its Mechanism for Chromium Removal | QU Min, WANG Yuan, CHEN Hui-xia, <i>et al.</i> (2370) |
| Mechanisms of Penicillin Wastewater Treatment by Coupled Electrocatalytic and Bioelectrochemical Systems | QU You-peng, LÜ Jiang-wei, DONG Yue, <i>et al.</i> (2378) |
| Aerobic Granular Sludge Operation and Nutrient Removal Mechanism from Domestic Sewage in an Anaerobic/Aerobic Alternating Continuous Flow System | LI Dong, YANG Jing-wei, LI Yue, <i>et al.</i> (2385) |
| In-situ Phosphorus Removal Activity and Impact of the Organic Matter Concentration on Denitrifying Phosphorus Removal in Sludge Aggregates | LÜ Yong-tao, JIANG Xiao-tong, TU Yan, <i>et al.</i> (2396) |
| In-situ Sludge Reduction Technology Based on Ozonation | XUE Bing, LIU Bin-han, WEI Ting-ting, <i>et al.</i> (2402) |
| Effects of Activated Carbon on the Fate of Antibiotic Resistance Genes During Anaerobic Digestion of the Organic Fraction of Municipal Solid Waste | MA Jia-ying, WANG Pan-liang, WANG Bing-han, <i>et al.</i> (2413) |
| Release Mechanisms of Carbon Source and Dissolved Organic Matter of Six Agricultural Wastes in the Initial Stage | LING Yu, YAN Guo-kai, WANG Hai-yan, <i>et al.</i> (2422) |
| Spatial Differentiation of Soil Organic Carbon Density and Influencing Factors in Typical Croplands of China | LI Cheng, WANG Rang-hui, LI Zhao-zhe, <i>et al.</i> (2432) |
| Characteristics of Paddy Soil Organic Carbon Mineralization and Influencing Factors Under Different Water Conditions and Microbial Biomass Levels | LIU Qi, LI Yu-hong, LI Zhe, <i>et al.</i> (2440) |
| Analysis of Nitrogen Transformation Characteristics and Influencing Factors of Forestland Soil in the Qinghai-Tibet Plateau; A Case Study of the Qilian Mountains and Southeast Tibet | HE Fang, ZHANG Li-mei, SHEN Cong-cong, <i>et al.</i> (2449) |
| Using the Matter-Element Extension Model to Assess Heavy Metal Pollution in Topsoil in Parks in the Main District Park of Lanzhou City | HU Meng-jun, LI Chun-yan, LI Na-na, <i>et al.</i> (2457) |
| Effects of Long-Term Application of Chemical Fertilizers and Organic Fertilizers on Heavy Metals and Their Availability in Reddish Paddy Soil | XIA Wen-jian, ZHANG Li-fang, LIU Zeng-bing, <i>et al.</i> (2469) |
| Characteristics and Origins of Heavy Metals in Soil and Crops in Mountain Area of Southern Sichuan | HAN Wei, WANG Cheng-wen, PNEG Min, <i>et al.</i> (2480) |
| Spatial Distribution Characteristics, Source Apportionment, and Risk Assessment of Topsoil PAHs in the Core Area of the Ningdong Energy and Chemical Industry Base | YANG Fan, LUO Hong-xue, ZHONG Yan-xia, <i>et al.</i> (2490) |
| Functional Stability and Applicability of Heavy Metal Passivators in Reducing Cd Uptake by Lettuce | PANG Fa-hu, WU Xue-jiao, KONG Xue-fei, <i>et al.</i> (2502) |
| Effects of Water Management on Cadmium Accumulation by Rice (<i>Oryza sativa</i> L.) Growing in Typical Paddy Soil | ZHANG Yu-ting, TIAN Ying-bing, HUANG Dao-you, <i>et al.</i> (2512) |
| Adsorption Properties of Oiltea Camellia Shell-Modified Biochar and Effects of Coupled Waterlogging on Soil Cd Morphology | CAI Tong, DU Hui-hui, LIU Xiao-li, <i>et al.</i> (2522) |
| Effects of Land Use Changes on Soil Fungal Community Structure and Function in the Riparian Wetland Along the Downstream of the Songhua River | XU Fei, ZHANG Tuo, HUAI Bao-dong, <i>et al.</i> (2531) |
| Distribution of Antibiotic Resistance Genes and Microbial Communities in a Fishery Reclamation Mining Subsidence Area | CHENG Sen, LU Ping, FENG Qi-yan (2541) |
| Effects of Three Commonly Used Herbicides on Bacterial Antibiotic Resistance | LI Xi, LIAO Han-peng, CUI Peng, <i>et al.</i> (2550) |
| Discussion of Microbial Control Standards of Water Reclamation and Formulation Methods | CHEN Zhuo, CUI Qi, CAO Ke-fan, <i>et al.</i> (2558) |